ELSEVIER

Biophysical Chemistry 55 (1995) 55–68

Biophysical Chemistry

The computer as a laboratory for the physical chemistry of membranes

O.G. Mouritsen [a,*,1], B. Dammann [a], H.C. Fogedby [b], J.H. Ipsen [a], C. Jeppesen [c], K. Jørgensen [a], J. Risbo [a], M.C. Sabra [a], M.M. Sperotto [a], M.J. Zuckermann [a,d]

[a] *Department of Physical Chemistry, The Technical University of Denmark, Building 206, DK-2800 Lyngby, Denmark*
[b] *Institute for Physics and Astronomy, Aarhus University, DK-8000 Aarhus C, Denmark*
[c] *Materials Research Laboratory, University of California, Santa Barbara, CA 93106, USA*
[d] *Centre for the Physics of Materials, McGill University, Montreal, PQ, H3A 2T8, Canada*

Abstract

A mini-review is given of some recent advances in the use of computer-simulation approaches to the study of physico-chemical properties of lipid bilayers and biological membranes. The simulations are based on microscopic molecular interaction models as well as random-surface models of fluid membranes. Particular emphasis is put on those properties that are controlled by the many-particle character of the lamellar membrane, i.e. correlations and fluctuations in density, composition and large-scale conformational structure. It is discussed how dynamic membrane heterogeneity arises and how it is affected by various molecular species interacting with membranes, such as cholesterol, drugs, insecticides, as well as polypeptides and integral membrane proteins. The influence of bending rigidity and osmotic-pressure gradients on large-scale membrane conformation and topology is described.

Keywords: Lipid bilayer; Phase transition; Fluctuation; Dynamic heterogeneity; Phase separation; Lipid mixture; Cholesterol; Insecticide; Lipid–protein interaction; Random surface; Bending rigidity; Membrane topology; Computer simulation

1. Introduction

The electronic computer is possibly the single most important invention that has had the most dramatic and lasting influence on the broadest range of experimental and theoretical disciplines in science. This holds true for both the fundamental as well as the more applied fields of science. Membrane science, and in particular, the physical chemistry of biological membranes are no exceptions.

The computer has found a quite remarkable use within the field of numerical simulation. In this field, it is employed as a piece of experimental equipment for the simulation and investigation of theoretical models describing a great variety of physical phenomena. Indeed, computer simulation of particle systems [1–3] has come to play a dominant role in modern science in general and in complex and soft condensed-matter physics in particular. In many cases it represents the only means of making quantitative progress in the study of a complex system or of a simple system with complex behavior. The particular

* Corresponding author.
[1] Associate fellow of The Canadian Institute of Advanced Research.

SSDI 0301-4622(94)00142-1

power of a computer-simulation approach is that it is conceptually simple and transparent, it builds on basic statistical mechanical concepts and it is very flexible as it allows us to adapt previously developed algorithms relatively easily to very different problems. Computer simulation, which may be seen as a type of a numerical experiment carried out on a well-defined system, lies between laboratory experiments and analytical theory. On the one hand it is an extremely useful way of testing the predictive power of specific models and the validity of theoretical approximations and on the other hand it can be carried out on quite realistic models. Computer simulation may therefore be used to interpret experimental data and may in this way be helpful in proposing further experimental investigations for a given system. In this interplay of theory and experiment, computer simulation is capable of providing clues to the relevant variables of a particular system or phenomenon. A special virtue of computer simulation is that it gives access to a description of the systems on the microscopic (molecular) level and that the accuracy of the results obtained is limited only by the available computer resources and by the level of details built into the model upon which the simulation is based.

The term computer simulation covers a wide range of computational techniques from stochastic (Monte Carlo) simulations for evaluation of physico-chemical equilibrium behavior to molecular-dynamics simulations that give direct access to the dynamic behavior. The different simulation techniques can be used to obtain both a general qualitative scaling behavior as well as detailed quantitative insight into material-specific properties. In the present paper we shall review some recent advances in the use of Monte Carlo simulation to study the physical properties of lipid bilayers and membranes using mainly results from our own work as examples. We shall show that both generic as well as material-specific information on membrane systems can be obtained from the simulations thereby illustrating the potential of the computer as a laboratory for the study of membrane systems.

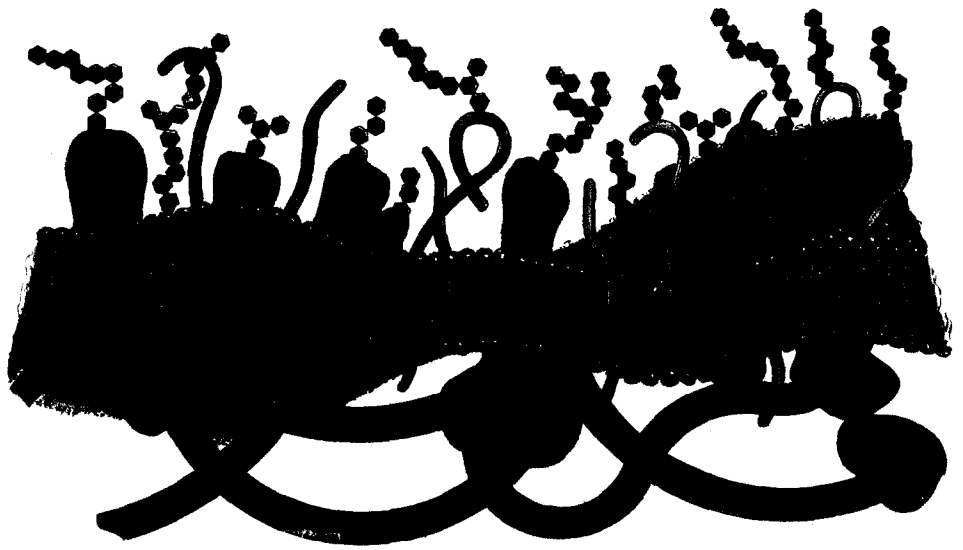

Fig. 1. Artist's conception of an eucaryotic plasma membrane showing the lipid-bilayer core, peripheral and integral membrane proteins, the cytoplasmatic cytoskeleton, and the carbohydrate glycocalyx on the outside surface. Under physiological conditions the membrane behaves like a pseudo-two-dimensional liquid. (Illustration by Ove Broo Sørensen, The Technical University of Denmark).

2. Lipid membranes and membrane models

Lipid bilayers vesicles, liposomes, and the lipid-bilayer component of biological membranes are mesoscopic systems consisting typically of 10^8–10^{10} interacting particles. A cartoon of a typical biological membrane is shown in Fig. 1. Such systems are therefore not represented by the thermodynamic limit and hence not truly macroscopic. They are, however, sufficiently large to sustain correlated dynamical modes and to display cooperative phenomena such as phase transitions, global phase separation, as well as dynamic nano-scale heterogeneity [4]. An example of the latter is the presence of fluctuating nano-scale clusters of an unstable phase in a stable phase. These phenomena are non-trivial consequences of the many-particle character of the system and its molecular interactions and they can neither be understood nor described in terms of the properties of the individual molecules alone. The cooperativity and the correlated modes of the membrane are manifested on many different length- and time-scales and they provide the main source of organization of the lipid bilayer. They are furthermore of seminal importance for describing the occurrence of differentiated regions such as lipid domains in the membrane [5,6].

It is in principle possible to write down a detailed and realistic model of a lipid-bilayer membrane which takes into account the microscopic molecular interactions between the different membrane constituents as well as the properties of the aqueous solvent and the ions. Statistical mechanics would then provide the connection between this microscopic model and the macroscopic, thermodynamic properties of the membrane. In practice, such an approach is not feasible and possibly not even desirable since it would produce an overwhelming amount of information which may tend to obscure the physical meaning. It is possible, however, to work with quite detailed membrane models if certain restrictions are made, particularly with respect to the number of molecules treated, i.e. the size of the membrane system, and the region of thermodynamic space considered, e.g. by confining the calculations to regions far from phase transitions.

Detailed information on the equilibrium properties and dynamics of lipid bilayers has been obtained from both Monte Carlo and molecular dynamics simulations on rather detailed membrane models which include the surrounding water molecules [7–11]. Even though these simulations are restricted to a few hundred lipid molecules they lead to important numerical data for acyl-chain order parameters and information on short-scale collective dynamic modes. Furthermore, the influence on the lipid structure due to the presence of membrane-associated molecules such as cholesterol, polypeptides and integral membrane proteins can be examined [12–14].

If the purpose of the simulations is to study phase transitions and bilayer structure on larger length scales, e.g. 100–1000 Å, using computer-simulation techniques it is necessary to work with simplified membrane models with coarse-grained variables and effective interaction potentials. Furthermore, the models should be formulated in terms of only a small number of mechanical variables. This is clearly a severe limitation of the approach. However, it may also be seen as a strength in the sense that such an approach may provide a means for determining those system variables that are the relevant ones for describing the particular phenomenon under consideration. Specifically, it is advantageous to work with a minimal set of variables when determining the generic and universal properties of a complex system.

Two types of simple membrane models have proved extremely useful for describing the physical properties of membrane systems that are strongly controlled by fluctuations. These two types attempt to describe the membrane properties at two different limits of the characteristic length scale of the system. The first type is concerned with the molecular organization, the structure and the dynamics of an essentially flat lipid-bilayer array [15,16] but neglects the fact that the lipid bilayer is a highly flexible and undulating surface. The second type attempts to describe the large-scale conformational complexity of the lipid membrane seen as a continuous surface imparted with a high degree of softness and flexibility, but without any specific molecular structure [17]. Ultimatively, the two types of membrane modelling should be unified into a single membrane model. Currently, such a unified model would be too complex for examination by computer-simulation techniques.

Selected results obtained from computer-simula-

tion calculations on these two types of membrane models are described below in Sections 3–7 and Section 8, respectively.

3. Lipid-bilayer phase transition: from microscopics to macroscopics

Phospholipid bilayers display a number of different phase transitions of which the main phase transition is biologically the most relevant one for lamellar bilayers [18]. The main transition, which is endothermic, takes the lipid bilayer from a solid-ordered or crystal phase with a high degree of acyl-chain conformational order to a fluid-disordered or liquid phase with acyl-chain conformational disorder. The internal entropy in the acyl chains provides the main driving force for this transition.

The transitional properties of lipid bilayers can be modelled by lattice models of the type used in statistical mechanics. One of these is a multi-state lattice model due to Pink [15,19] which has proved to be useful in the analysis of the properties of lipid systems. In the Pink model only a small number of selected acyl-chain conformational states are considered. The model, which is analyzed using a triangular lattice and accounts for both the acyl-chain conformational statistics and the van der Waals interactions between the chains, is defined by the following Hamiltonian

$$\mathscr{H} = \Pi \sum_i A_i + \mathscr{H}_{cc} \qquad (1)$$

where the sum is over all molecules. Π is an interfacial lateral pressure that assures bilayer stability. The van der Waals interactions between acyl chains are denoted by $\mathscr{H}_{cc}$ which can be formulated in terms of the cross-sectional areas, A_i, of the individual acyl chains. The value of the molecular area reflects the degree of acyl-chain conformational order. For a bilayer phase where the averaging of the molecular motions takes place around the bilayer normal, there is an inverse linear relationship between the average cross-sectional membrane area per molecule, $\langle A \rangle$, and the conformational acyl-chain order parameter, S [20] defined as the average segmental order parameter

$$S = \left\langle 3\cos^2\theta - \tfrac{1}{2} \right\rangle = a_1 \langle A \rangle^{-1} + a_2 \qquad (2)$$

where a_1 and a_2 are geometric constants.

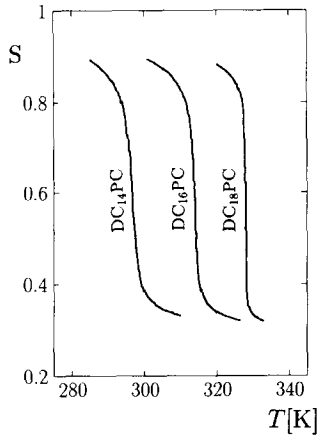

Fig. 2. Computer-simulation data for the average acyl-chain order parameter, $S(T)$ in Eq. (2), as a function of temperature for $DC_{14}PC$, $DC_{16}PC$ and $DC_{18}PC$ bilayers.

In Fig. 2 are shown the results for S for three different saturated di-acyl phospholipid bilayers [2] obtained form Monte Carlo simulations on the Pink model. The data show an abrupt decrease of the acyl-chain order in a narrow temperature region around a transition temperature, T_m, whose value increases linearly with acyl-chain length. The transition becomes more abrupt as the acyl-chain length increases, in agreement with recent H^2-NMR experiments [21]. The specific heat, $C(T)$, for the same series of lipids is shown in Fig. 3. In computer simulations, response functions such as the specific heat can readily be determined via the fluctuation-dissipation theorem

$$C(T) = \frac{1}{k_B T^2}\left(\langle \mathscr{H}^2 \rangle - \langle \mathscr{H} \rangle^2\right) \qquad (3)$$

Fig. 3 shows that the specific heat exhibits a strong anomaly in the transition region. The most remarkable feature of this data set is the presence of substantial wings in the specific heat away from the transition, signalling strong fluctuations-induced precursor effects. Fig. 3 also shows that the fluctuations become stronger with decreasing acyl-chain length, Hence the phase transition is not the usual type of

[2] Abbreviations: DC_nPC: di-acyl phosphatidylcholine with n carbon atoms in each acyl chain; NMR: nuclear magnetic resonance.

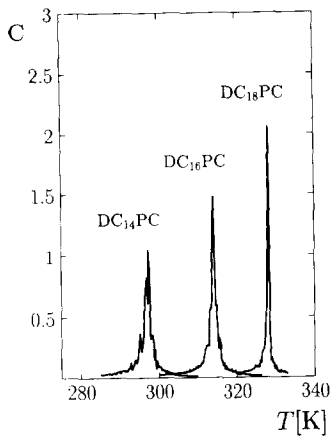

Fig. 3. Computer-simulation data for the specific heat, $C(T)$, as a function of temperature for $DC_{14}PC$, $DC_{16}PC$ and $DC_{18}PC$ bilayers. C is in units of 10^{-13} erg.

first-order transition associated with a delta-function singularity in the specific heat, but instead there is a substantial amount of heat in the wings. These findings are in agreement with the most precise equilibrium measurements of the specific heat by differential-scanning calorimetry [22] which indicates that most of the transitional heat is associated with the wings of the specific heat. This may indicate that the main transition is either a very weak first-order transition or no transition at all in a strict thermodynamic sense (see also Section 4). Both the experimental observations and the simulation data point to the possibility that the bilayer transition is pseudo-critical in the sense that the transition is very close to a critical point and hence dominated by strong density fluctuations [16,21,23,24].

When the computer is used as a laboratory to study the physical chemistry of membranes, bulk macroscopic properties like order parameters and response functions are not the only properties which can be determined. Indeed, since the computer deals directly with the microscopic variables of the system, in this case the acyl-chain conformational states, it is possible to obtain information on the microscopic level, in particular about the lateral organization of the bilayer. In Fig. 4 are shown examples of this type of information for temperatures in the fluid phase just above the main transition for the three different lipids [6]. The figure shows that the strong fluctuations detected in the specific heat manifest themselves on the microscopic and nanoscopic length scales via the formation of dynamic clusters or domains of conformationally ordered lipids in the bulk fluid phase. Similarly, below the transition fluid lipid domains are formed in the solid phase [25]. These domains are dynamic entities characterized by a specific temperature-dependent size distribution. The domains never grow to macroscopic size (except at the transition point) and their presence therefore does not correspond to bulk phase separation. We characterize this state of the bilayer in the transition region as a dynamic heterogeneous state [26,27]. Fig. 4 shows that the degree of dynamic heterogeneity increases as the acyl-chain length decreases.

The dynamic heterogeneity and domain formation phenomena in the transition region of lipid bilayers

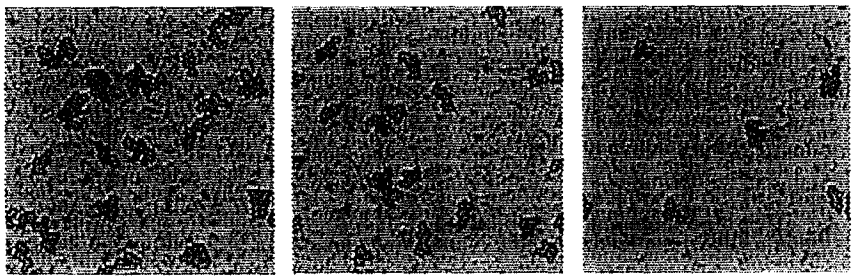

Fig. 4. Computer-generated snapshots of typical lateral configurations of $DC_{14}PC$, $DC_{16}PC$ and $DC_{18}PC$ bilayers (seen from above) at the same relative temperature, $T/T_m = 1.016$, in the fluid phase. Each snapshot corresponds to a system of 5000 lipid molecules. Solid and fluid regions are shown in grey and white tones, and the interfaces between the solid lipid domains and the bulk fluid phase are highlighted in black.

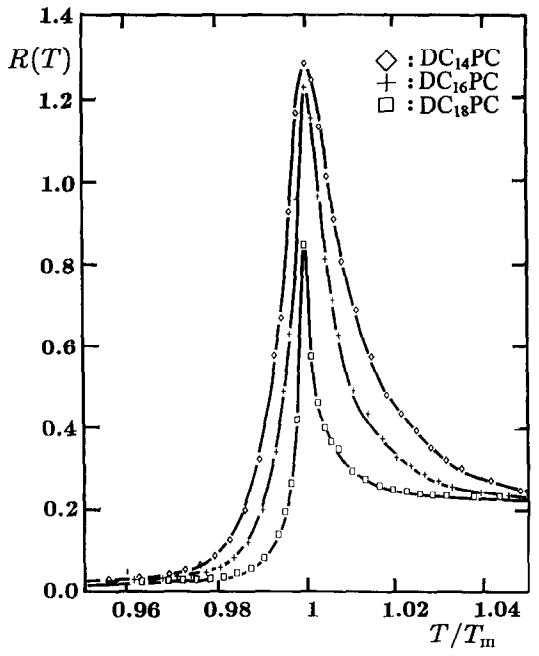

Fig. 5. Computer-simulation data for the relative permeability, $R(T)$ in Eq. (4), of $DC_{14}PC$, $DC_{16}PC$ and $DC_{18}PC$ bilayers as a function of reduced temperature, T/T_m, where T_m is the transition temperature of the lipid in question.

have a number of striking consequences for both passive and active functions that take place in association with membranes, such as passive permeability and enzyme action [22,26,27]. In Fig. 5 are shown some results for the passive permeability of small ions, such as Na^+, derived from Monte Carlo simulation data of the type shown in Fig. 4 using a simple model that associates high transmission coefficients to the area of the lipid bilayer that bounds the lipid domains and the bulk [28,29]. Within this model the relative permeability is expressed as

$$R(T) = \langle A(T) \rangle^{-1/2} T^{1/2} \left(a_b(T) p_b + a_c(T) p_c + a_i(T) p_i \right) \quad (4)$$

where the major temperature dependence is contained in the fractional areas, a_b, a_c, a_i, of the bulk, the clusters and their mutual interface. It can be seen from Fig. 5 that a sharp permeability anomaly is predicted in the transition region, which is in quantitative agreement [28] with experimental observations [30,31].

4. Phase equilibria in lipid mixtures

Phase transitions in one-component systems are relatively easily detected by experimental observations of order parameters and response functions which display anomalies at phase transitions, both first-order transitions and critical points. However, when it comes to mixtures the lack of information on the level of the free energy becomes problematic. First and second derivatives of the free energy, such as order parameters and response functions, may be difficult to interpret in terms of phase equilibria and consequently an accurate determination of phase diagrams is hampered. This is particularly troublesome the more ideal the mixture is. Furthermore, many experimental techniques used to study lipid membranes involve local probes of some kind such as magnetic resonance or fluorescence. In principle, such techniques can not distinguish between the occurrence of global phase separation and the presence of lipid domains that persist on a length scale larger that the length over which the probe can diffuse during the characteristic time of observation.

Conventional computer-simulations studies of phase equilibria suffer from the same shortcomings as the laboratory experiments since they usually lead to information about derivatives of the free energy. Recently some novel techniques have been proposed that involve thermodynamic reweighing and finite-size scaling analysis of the computer-generated data [32–35]. In the case of a binary mixture, the idea is first to calculate distribution functions, $\mathscr{P}(x,T,L)$, for the composition, x, of the mixture for a series of finite systems of linear extension, L, at a given chemical potential, μ. The distribution function can be reweighed so as to tune in to the value of the chemical potential corresponding to phase coexistence at the given temperature. Secondly, one studies the free-energy analogue, $\mathscr{F}(x,T,L) \sim -\ln \mathscr{P}(x,T,L)$, which differs from the total free energy by a temperature- and size-dependent term. Hence differences in $\mathscr{F}$ for the same temperature and the same system size are correct measures of free-energy differences that can be used to determine the relative stability of different phases. Specifically, for a system at a phase transition where a barrier

$$\Delta \mathscr{F}(\mu,T,L) \sim \gamma(\mu,T) L^{d-1} \quad (5)$$

between the two phases develops, the nature of the transition and hence the position of the phase boundary can be assessed by studying the size-dependence of the barrier. For a first-order transition the barrier between the coexisting phases scales as L^{d-1}, where d is the spatial dimension, and the proportionality constant, γ, is the interfacial tension.

An example of use of this type of analysis to simulation data derived for the binary lipid mixture $DC_{14}PC$–$DC_{18}PC$ using the Pink model for a planar lipid bilayer [35] is given in Fig. 6. The free-energy function in Fig. 6a clearly shows that the barrier between the two phases increases (linearly) with system size for the composition under consideration. The resulting phase diagram for the mixture in the complete composition range is shown in Fig. 6b. A strong phase separation is observed signalling a highly non-ideal character, in good agreement with the interpretation of experimental data [36]. However, the diagram also shows that the coexistence region is a closed loop with two critical mixing points. This particular feature is caused by the fact that the model used to describe the pure $DC_{14}PC$ and $DC_{18}PC$ bilayers, which is the same model as described in Section 3 above, does not display a phase transition in a strict thermodynamic sense for the values of the parameters used in the simulations. For these parameters, the system is beyond a critical point, although very close [35,37]. For all practical purposes the bilayer behaves as though it has undergone a phase transition. Experimentally, however, it is virtually impossible to determine whether this is the case or not. The fact remains that there is no single piece of experimental evidence which has unequivocally demonstrated that pure phospholipid bilayers do indeed exhibit a phase transition in a strict thermodynamic sense. The computer-simulation calculations suggest that the longer the acyl chain length the more likely it is that the bilayer undergoes a first-order transition [35,37].

5. Cholesterol and lipid order

Investigations into the physical chemistry of lipid–cholesterol mixtures have turned out to be quite difficult [38,39], probably because cholesterol molecules interact very differently with the confor-

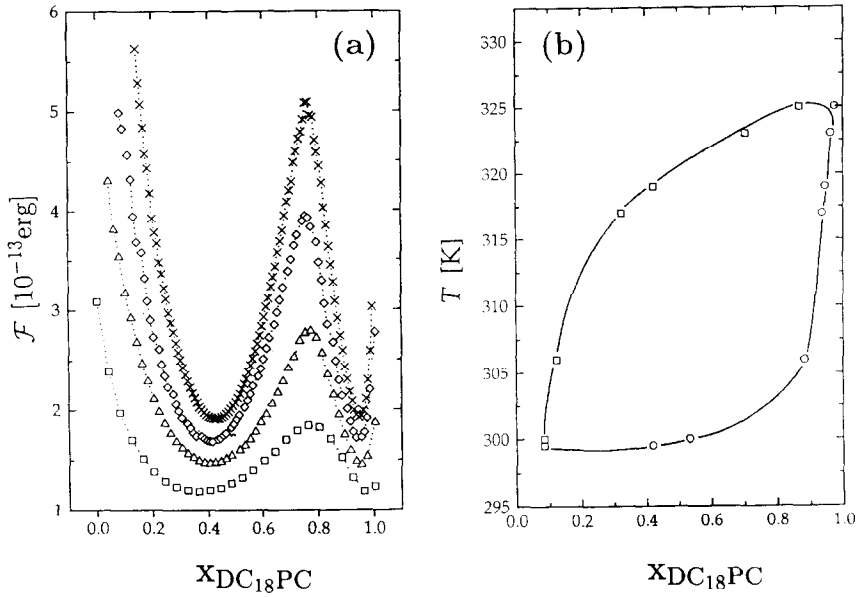

Fig. 6. Computer-simulation data characterizing the phase behavior of a $DC_{14}PC$–$DC_{18}PC$ mixture in a lamellar bilayer. (a) The size-dependence of the free-energy function $\mathcal{F}(x,L)$ calculated at coexistence, $\mu(L)$, at the temperature $T = 319$ K. The linear sizes of the bilayer systems correspond to $L = 5$ (□), 7 (△), 9 (◇), and 11 (×). (b) The phase diagram in the T-x-plane.

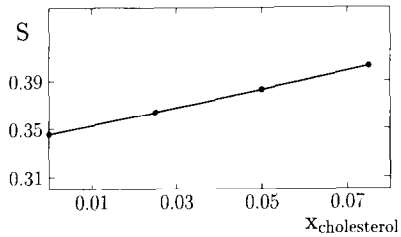

Fig. 7. Computer-simulation data for the average acyl-chain order parameter, S, for a $DC_{16}PC$ bilayer at a temperature, $T = 319$ K, in the fluid phase incorporated with different amounts of cholesterol.

mational and translational degrees of freedom of the lipid molecules in a lamellar bilayer. It has been shown that large concentrations of cholesterol promote a new bilayer phase, the liquid-ordered phase [38], which is a liquid that can simultaneously be characterized by a high degree of acyl-chain conformational order. At low concentrations the effects of cholesterol on the lipid-bilayer phase behavior are quite subtle [38,40,41]. Contrary to the situation at high concentrations, cholesterol at low concentrations enhances the thermal fluctuations of the bilayer and is found experimentally as well as by computer simulations to increase the passive permeability [41].

The effect of cholesterol on the acyl-chain conformational order parameter, S, for $DC_{16}PC$ bilayers at a temperature in the fluid phase is shown in Fig. 7. The data was obtained from simulations on an extension of the Pink model which takes into account the van der Waals interactions between the flexible chains of the phospholipids with the rigid sterol skeleton of cholesterol. An ordering effect due to cholesterol is clearly seen in this figure. This is in good agreement with experimental measurements of the order by ^{2}H-NMR spectroscopy [39].

6. Drug molecules and insecticides in lipid bilayers

Binary lipid mixtures and lipid–cholesterol mixtures can be considered from the standpoint of physical chemistry as substitutional alloys due to the compatibility between the sizes and the amphiphilicity of the molecules of the mixtures. There are, however, several classes of foreign molecules which interact with bilayer membranes and form interstitial alloys with the lipid molecules. In these systems the incorporated foreign molecules act thermodynamically as though they have effectively zero specific volume. One implication of this behavior is that the entropy of mixing is vanishingly small. Examples of such classes of foreign molecules are certain anaesthetics like halothane and dibucaine, and organochloric insecticides such as lindane and DDT.

Recently, computer simulations on simple lattice models were used as a laboratory to study the interaction of interstitially intercalating foreign molecules with lipid bilayers [42–45]. The ultimate goal of such studies is to understand the physical aspects of the molecular mechanism of anaesthesia and the effect of pesticides on neural membranes. The models used are extensions of the Pink lattice model which allows interstitial lattice sites to be occupied by the foreign molecules and the exchange of these molecules with an aqueous reservoir controlled by a chemical potential.

In Fig. 8 are shown data obtained from such calculations for the partition coefficient [43], $x(T)$, and the fluctuation of the partition coefficient, $\chi(T) = \langle x^2(T)\rangle - \langle x(T)\rangle^2$ in the case of a water-soluble drug like halothane or an insecticide like lindane. $x(T)$ is a measure of the relative amount of the foreign molecules adsorbed in the lipid bilayer and $\chi(T)$ measures the compositional fluctuations in the doped bilayer. It is observed from Fig. 8a that the partition coefficient has a peak near the phase transition of the lipid bilayer. This is a non-classical effect which shows that there is a fluctuation-induced enhancement of the adsorption in the transition region. The corresponding effect in the specific heat is a broadening and a shift to lower temperatures [43]. These general observations are in agreement with experimental studies of halothane and dibucaine [46,47] as well as lindane and DDT [48,49] interacting with lipid bilayers, and a number of other systems [43,44]. Concomitant with the enhanced adsorption near the transition the compositional fluctuations shown in Fig. 8b display a dramatic peak. The quantity $\chi(T)$ is an example of a property which can readily be obtained from a computer experiment but is not so easily obtained from a conventional laboratory experiment.

The effect of partitioning of lindane in phospholipid bilayers of different chain lengths as obtained

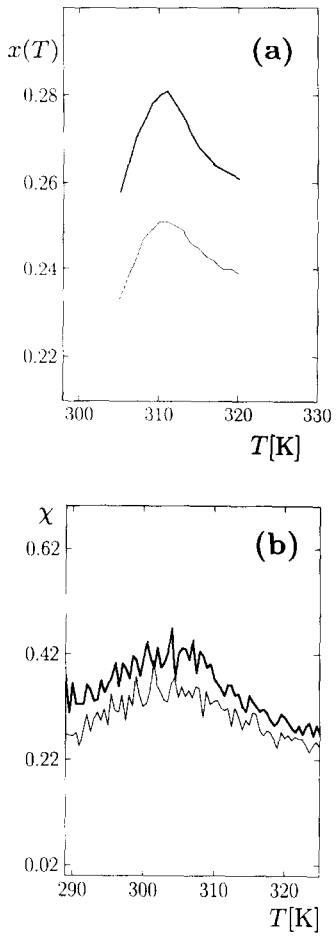

Fig. 8. Computer-simulation data for (a) the partition coefficient, $x(T)$, and (b) the compositional fluctuations, $\chi = \langle x^2 \rangle - \langle x \rangle^2$, of a water-soluble drug like halothane dissolved in a $DC_{16}PC$ bilayer (heavy solid line) and a $DC_{16}PC$ bilayer incorporated with 10% cholesterol (thin solid line).

from computer simulations is illustrated in Fig. 9 [45]. The chemical potential in these calculations is adjusted to account for the different solubilities of lindane in the different bilayers. The data shows that the enhanced adsorption peak tracks the phase transition and that the effect is more pronounced in the bilayers with shorter acyl chains, in agreement with experimental measurements [48,49]. This is consistent with the result [43] that the degree of bilayer dynamic heterogeneity correlates with the adsorption of insecticides.

7. Lipid–polypeptide and lipid–protein interactions

It has been suggested that one aspect of lipid–protein interactions is the degree of matching between the hydrophobic bilayer thickness and the hydrophobic length of the membrane-spanning protein or amphiphilic polypeptide [50,51]. The concept of hydrophobic matching has been built into the microscopic interaction models of lipid bilayers [52], Eq. (1), and has been used to determine a variety of properties of lipid–protein systems, such as phase equilibria, protein aggregation, and conformational and compositional lipid profiles near the protein.

In Fig. 10 are shown data for the specific heat and the phase diagram obtained from a computer simulation for a mixture of $DC_{16}PC$ with the amphiphilic polypeptide lys_2-gly-leu_{24}-lys_2-ala-amide [52]. The techniques used to derive the phase diagram from the simulation data were already described in Section 4 for binary lipid mixtures. The phase diagram, which displays a closed coexistence region and a lower critical mixing point, is in good agreement with the experimental phase diagram obtained from ^{2}H-NMR

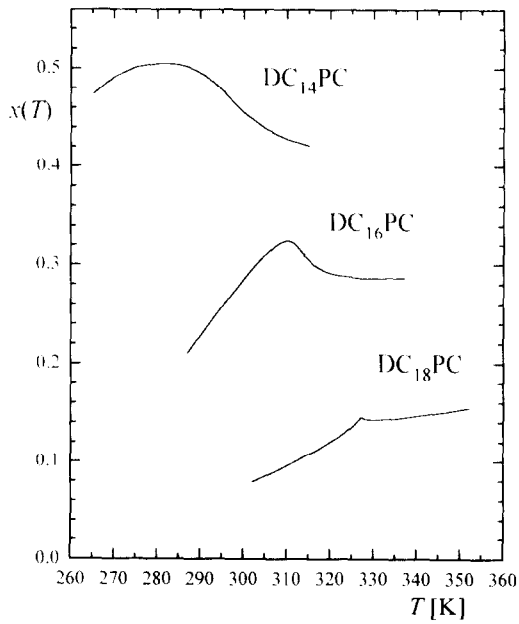

Fig. 9. Computer-simulation data for the partition coefficient, $x(T)$, of a water-soluble insecticide like lindane dissolved in $DC_{14}PC$, $DC_{16}PC$ and $DC_{18}PC$ bilayers.

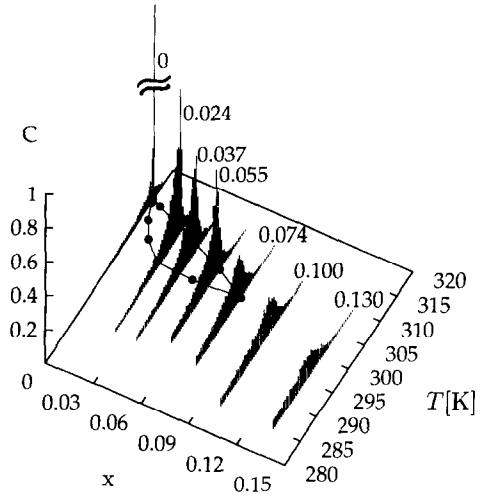

Fig. 10. Computer-simulation data for the specific heat, $C(x,T)$, as a function of composition, x, and temperature for a $DC_{16}PC$ bilayer incorporated with trans-bilayer amphiphilic polypeptides of the type lys_2-gly-leu_{24}-ala-amide. C is in units of 10^{-13} erg. The corresponding phase diagram is shown in the x-T-plane.

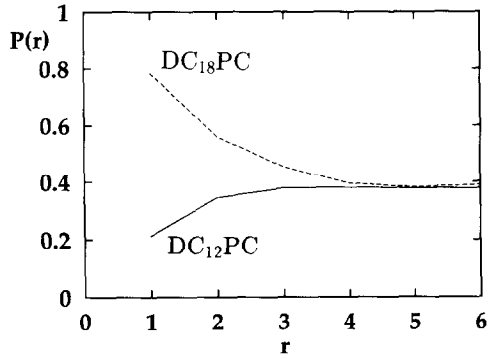

Fig. 12. Computer-simulation data for the lipid compositional profiles, $P(r)$ (in units of lipid-acyl-chain diameters), in a 1:1 $DC_{14}PC$–$DC_{18}PC$ mixture in a fluid lamellar bilayer at $T = 325$ K incorporated with a model integral protein resembling bacteriorhodopsin. C is in units of 10^{-13} erg.

difference spectroscopy [53]. The data shown in Fig. 10 are an excellent illustration of the difficulties that may arise when one tries to derive phase diagrams from measurements of the specific heat alone. Obviously, due to the critical mixing point the specific heat displays a strong peak even in the region where the mixture is in a single thermodynamic phase. Such a peak could mistakenly be interpreted to signal a phase transition.

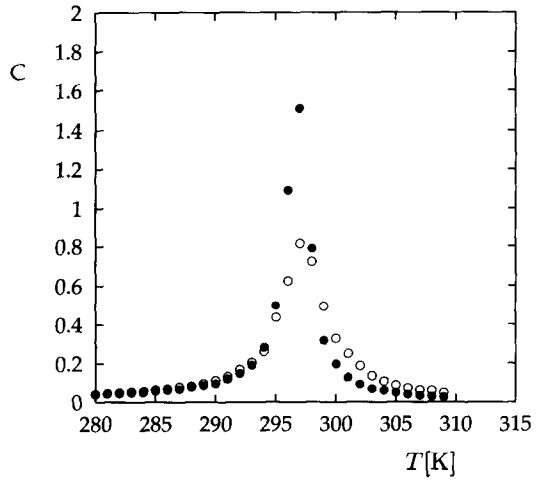

Fig. 11. Computer-simulation data for the specific heat, $C(T)$, of a $DC_{16}PC$ bilayer incorporated with a model integral protein resembling bacteriorhodopsin (○). The specific-heat data for the pure $DC_{16}PC$ bilayer are shown for comparison (●). C is in units of 10^{-13} erg.

The effect of a larger protein, such as bacteriorhodopsin, on the specific heat of a $DC_{14}PC$ lipid bilayer is shown in Fig. 11 [54]. In this case the hydrophobic length of the protein matches slightly better with the hydrophobic thickness of the solid phase of the lipid molecules. This leads to a freezing-point elevation and a concomitant broadening of the specific heat corresponding to a phase-separation region. These observations are in agreement with experimental data from differential scanning calorimetry [55].

An interesting effect arises when a integral membrane protein is dissolved in a binary lipid mixture in which the two lipid species have different affinities for the protein due to different fulfilments of the hydrophobic-matching condition [54]. A local demixing of the two species then occurs as shown in Fig. 12 for bacteriorhodopsin in a $DC_{12}PC$–$DC_{18}PC$ mixture in the fluid phase. This is a case of physical selectivity or lipid specificity. It should be noted that the profiles shown in Fig. 12 are statistical measures and there is no specific binding of lipid molecules to the protein.

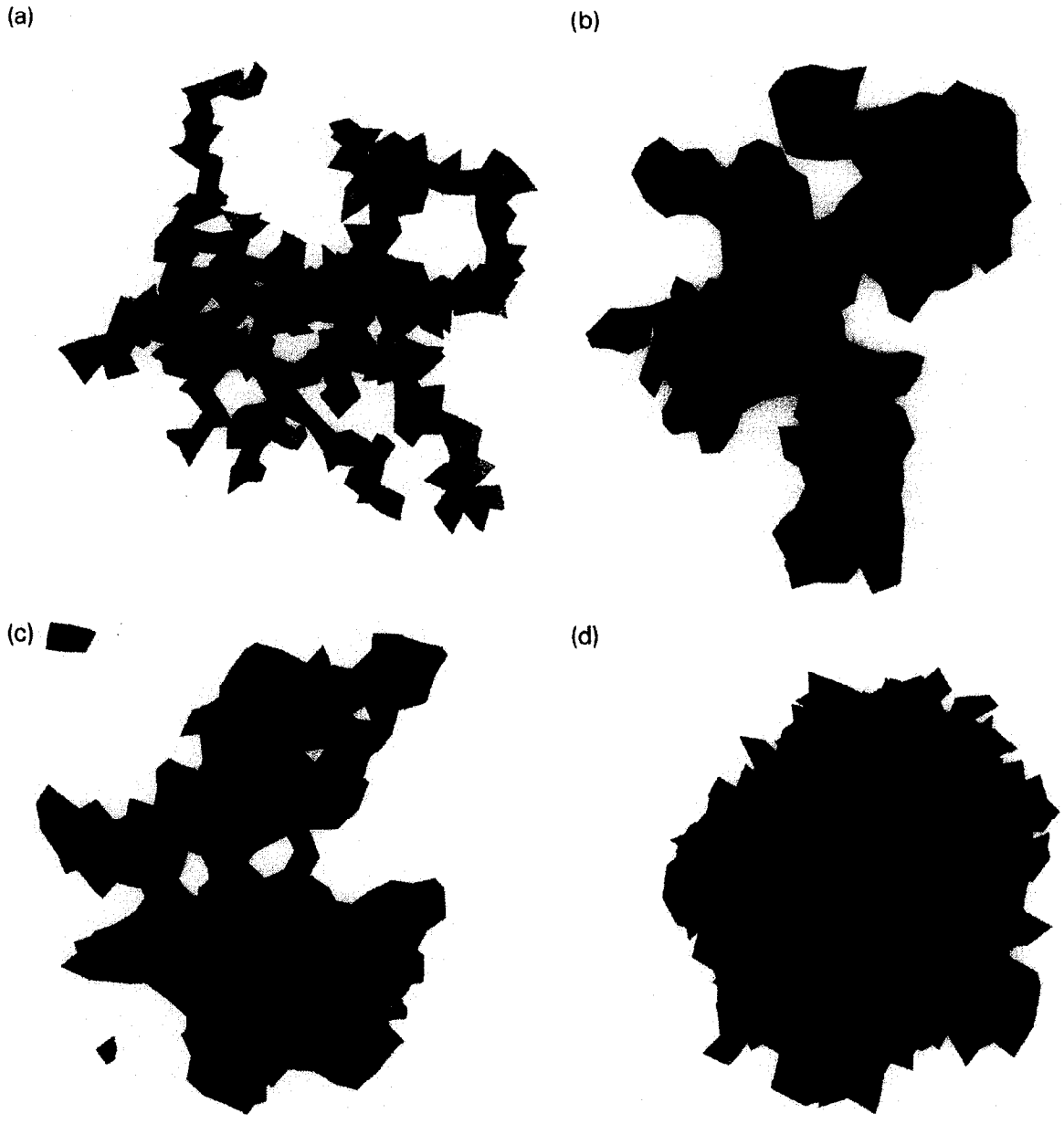

Fig. 13. Computer-generated illustrations of conformations of dynamically triangulated random surfaces resembling lipid bilayer membranes in the fluid state. (a) Branched-polymer configuration of a random closed surface of spherical topology with zero bending rigidity. (b) Short-scale compact and large-scale branched-polymer configuration of a random closed surface of spherical topology with a small bending rigidity. (c) Ensemble of closed random surfaces with free topology and a finite bending rigidity. (d) Inflated, crumpled state of a random closed surface of sperical topology and zero bending rigidity. The inflated state is induced by an osmotic pressure gradient.

8. Large-scale membrane conformations and topology

Upto this point we treated the lipid bilayer membrane as though it were inherently flat and on length scales where the size of the individual lipid molecules is essential. The softness of the bilayer only entered via the lateral compressibility of the bilayer. However, real bilayer membranes display large-scale conformational out-of-plane excursions (see Fig. 1) and there is an explicit coupling between the lateral compressibility modulus and the elastic bending rigidity [56]. The conformational structure of the membrane, when it is considered to be a flexible surface on scales larger than the molecular scale, is dominated by the fact that the interfacial tension is very low. The membrane properties are then controlled by the conformational entropy and the bending rigidity.

Self-avoiding random surfaces [57] are model systems for flexible membranes. On length scales much larger than those characterizing the individual molecules, the energetics of such objects can be described in terms of surface invariants like area, mean curvature and Gaussian curvature [58] according to the functional

$$\mathscr{H}/k_BT = \frac{\kappa}{2}\int \mathrm{d}A\left(\frac{1}{R_1}+\frac{1}{R_2}\right)^2 + \frac{\bar{\kappa}}{2}\int \mathrm{d}A\,\frac{2}{R_1R_2} - p\int \mathrm{d}V \qquad (6)$$

where R_1 and R_2 are the principal radii of curvature and κ and $\bar{\kappa}$ are the bending rigidity and the Gaussian curvature modulus respectively. The Gauss–Bonnet theorem implies that the Gaussian curvature term in Eq. (6) is equal to $\bar{\kappa}2\pi\chi_E$, where χ_E is the Euler characteristic of the surface, i.e. it determines the topology of the surface. In Eq. (6) the pressure, p, couples to the volume, V, of the closed membrane. In order to treat systems described by the continuum model in Eq. (6) by computer simulation it is necessary to discretize the model. Such a discretization is implemented via a triangulation of the surface. In order to determine thermodynamic properties of the discretized model it is necessary to sample over the totality of possible triangulations. During the sampling, the triangulation is updated dynamically in such a way as to keep the bilayer in the fluid phase. This is done by allowing the number of nearest-neighbor contacts between the nodes of the triangulation to fluctuate. The self-avoidance in the discrete model is enforced by choosing appropriate constraints involving a hard-core potential [59].

In Fig. 13 are shown examples of surface configurations derived from this type of model under a variety of conditions. Fig. 13a illustrates that the stable state of a fully flexible self-avoiding surface of spherical topology and zero bending rigidity is related to that of a branched polymer [61]. In this state, the surface has degenerated into a system of connected tubular surface elements. When a finite bending rigidity is introduced, the surface is characterized by a certain value of the persistence length [61] below which the membrane state is compact and above which there is a cross-over to the branched-polymer phase. It can be shown that the persistence length varies exponentially with the bending rigidity [61]. Hence, fluid membranes with finite bending rigidity should always display properties characteristic of branched polymers at large length scales. For plasma membranes that contain large concentrations of cholesterol and hence are very rigid, the persistence length is larger than the size of the cell and these membranes will therefore remain compact. This is not necessarily true of inner membranes which are much softer partly due to the absence of sterols. An example of a random surface of spherical topology with finite bending rigidity is shown in Fig. 13b. If the topology is now allowed to vary [59], yet more complex surface configurations occur, an example of this is shown in Fig. 13c. From calculations of this type it is in principle possible to calculate generic properties of vesicle-size distribution functions. Membrane topologies different from simple spherical topology occur in a number of different situations in biological systems. The convoluted membranes and their dynamic alteration in the Golgi apparatus form just one example.

It is possible to induce a transition from the branched-polymer phase (deflated phase) to an inflated phase by applying an osmotic pressure gradient across a closed spherical surface [60]. In Fig. 13d is shown an example of an inflated (crumpled) surface configuration of a random surface of spherical

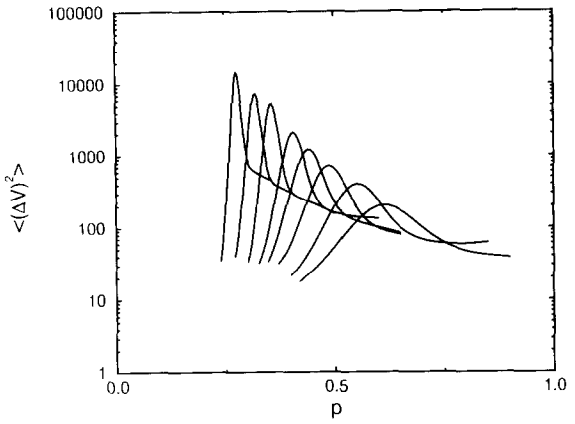

Fig. 14. Computer-simulation data for the volume fluctuations, $\langle(\Delta V)^2\rangle$ in Eq. (7), of a random triangulated closed membrane surface (vesicle) with zero bending rigidity, cf. Eq. (6). Data are displayed as a function of osmotic pressure, p, for a series of different vesicle sizes, $N = 11^2$, 12^2, 13^2, 14^2, 15^2, 16^2, 18^2, 20^2, going from right to left.

topology with zero bending rigidity. The volume fluctuations,

$$\langle(\Delta V)^2\rangle = \langle V^2\rangle - \langle V\rangle^2 \qquad (7)$$

of such a surface which depend on the osmotic pressure, p, are shown in Fig. 14 as a function of the size of the vesicle. The size, N, is here defined as the number of nodes in the triangulated network. It can be seen that the volume fluctuations, which are related to the compressibility, display a peak at the inflation–deflation transition pressure, $p = p^*$. Furthermore, this peak moves towards lower values of the pressure as the vesicle size increases. This variation can be expressed in terms of a scaling relation, $p^* \sim N^{-\alpha}$, with $\alpha = 0.69$ [60]. The peak intensity at the transition pressure obeys a different scaling relation, $\langle(\Delta V)^2(p = p^*)\rangle \sim N^{\gamma}$ with $\gamma = 3.62$.

Computer simulations on random surfaces are very demanding due to the large-scale conformational complexity of fluid flexible membranes. However, in the near future it should be possible to perform simulations on models that incorporate large-scale structure as well as molecular details. The computer will then have developed into an yet more interesting and useful laboratory for the study of the physical chemistry of membranes.

Acknowledgements

This work was supported by the Danish Natural Science Research Council under grants 11-0065-1 and 11-9560-1, the Danish Technical Research Council under grant 16-5039-1, by Jenny Vissings Fond, by the Carlsberg Foundation, by le FCAR du Quebec under a centre and team grant, and by NSERC of Canada. MJZ's sabattical leave in Denmark was supported by the Danish Research Academy under grant S940049.

References

[1] O.G. Mouritsen, Computer Studies of Phase Transitions and Critical Phenomena, Springer Verlag, Heidelberg, 1984.
[2] D.W. Heermann, Computer Simulation Methods in Theoretical Physics, Springer Verlag, Heidelberg, 1986.
[3] W.F. van Gunsteren, P.K. Weiner and A.J. Wilkinson, Computer Simulation of Biomolecular Systems: Theoretical and Experimental Applications, ESCOM, Leiden, 1993.
[4] O.G. Mouritsen and K. Jørgensen, Mol. Membrane Biol., (in press, 1995).
[5] K. Jacobson and W.L.C. Vaz, Comments Mol. Cell. Biophys., 8 (1992) 1.
[6] O.G. Mouritsen and K. Jørgensen, Chem. Phys. Lipids, 73 (1994) 3.
[7] H.C. Berendsen, in G. Ciccotti and W.G. Hoover (Editors), Proc. Int. Sch. Enrico Fermi, Course XCVII, North-Holland, Amsterdam, 1986, p. 496.
[8] P. van der Ploeg and H.J.C. Berendsen, Mol. Phys., 49 (1983) 233.
[9] S.-J. Marrink, M. Berkowitz and H.C. Berendsen, Langmuir, 9 (1993) 3122.
[10] H.L. Scott, in R. Brasseur (Editor), Molecular Description of Biological Membrane Components by Computer Aided Conformational Analysis, Vol. 1, CRC Press, Boca Raton, Florida, 1990, p. 123.
[11] H. Heller, M. Schaefer, and K. Schulten, J. Phys. Chem., 97 (1993) 8343–8360.
[12] H.L. Scott, J. Chem. Phys., 67 (1986) 6122.
[13] O. Edholm and J. Johansson, Eur. Biophys. J., 14 (1987) 203.
[14] O. Edholm, A.M. Nyberg and F. Jähnig, Biophys. Chem., 30 (1988) 279.
[15] O.G. Mouritsen, in R. Brasseur (Editor), Molecular Description of Biological Membrane Components by Computer Aided Conformational Analysis, Vol. 1, CRC Press, Boca Raton, Florida, 1990, p. 3.
[16] O.G. Mouritsen, Chem. Phys. Lipids, 57 (1991) 179.
[17] D. Nelson, in H.E. Stanley and N. Ostrowsky (Editors), Random Fluctuations and Pattern Growth: Experiments and Models, Kluwer Academic Publishers, Dordrecht, 1988, p. 193.

[18] P.K.J. Kinnunen and P. Laggner, Special Issue on Phospholipid Phase Transitions, Chem. Phys. Lipids, 57 (1991) 109.
[19] D.A. Pink, T.J. Green and D. Chapman, Biochemistry, 19 (1980) 349.
[20] J.H. Ipsen, O.G. Mouritsen and M. Bloom, Biophys. J., 57 (1990) 405.
[21] M.R. Morrow, J.P. Whitehead and D. Lu, Biophys. J., 63 (1992) 18.
[22] R.L. Biltonen, J. Chem. Thermodyn., 22 (1990) 1.
[23] O.G. Mouritsen and M.J. Zuckermann, Eur. Biophys. J., 12 (1985) 75.
[24] I. Hatta, S. Imaizumi and Y. Akutsu, J. Phys. Soc. Japan, 53 (1984) 882.
[25] J.H. Ipsen, K. Jørgensen and O.G. Mouritsen, Biophys. J., 58 (1990) 1099.
[26] O.G. Mouritsen and K. Jørgensen, Bioessays, 14 (1992) 129.
[27] O.G. Mouritsen and R.L. Biltonen, in A. Watts (Editor), Protein–Lipid Interactions. New Comprehensive Biochemistry, Vol. 25, 1993, p. 1.
[28] L. Cruzeiro-Hansson and O.G. Mouritsen, Biochim. Biophys. Acta, 944 (1988) 63.
[29] O.G. Mouritsen, K. Jørgensen and T. Hønger, in E.A. Disalvo and S.A. Simon (Editors), Permeability and Stability of Lipid Bilayers, CRC Press, Boca Raton, Florida, 1994, p. 89.
[30] D. Papahadjopoulos, K. Jacobson, S. Nir and T. Isac, Biochim. Biophys. Acta, 311 (1973) 330.
[31] A. Georgallas, J.D. MacArthur, X.-P. Ma, C.V. Nguyen, G.R. Palmer, M.A. Singer and M.Y. Tse, J. Chem. Phys., 86 (1987) 7218.
[32] A.M. Ferrenberg and R.H. Swendsen, Phys. Rev. Lett., 61 (1988) 2635.
[33] J. Lee and J.M. Kosterlitz, Phys. Rev. B, 43 (1991) 3265.
[34] Z. Zhang, O.G. Mouritsen and M.J. Zuckermann, Mod. Phys. Lett. B, 7 (1993) 217.
[35] J. Risbo, M.M. Sperotto and O.G. Mouritsen, (preprint, 1995).
[36] S. Mabrey and J.M. Sturtevant, Proc. Natl. Acad. Sci. USA, 73 (1976) 3862.
[37] E. Corvera, M. Laradji and M.J. Zuckermann, Phys. Rev. E, 47 (1993) 696.
[38] J.H. Ipsen, G. Karlström, O.G. Mouritsen, H. Wennerström and M.J. Zuckermann, Biochim. Biophys. Acta, 905 (1987) 162.
[39] M.R. Vist and J.H. Davis, Biochemistry, 29 (1990) 451.
[40] L. Cruzeiro-Hansson, J.H. Ipsen and O.G. Mouritsen, Biochim. Biophys. Acta, 979 (1989) 166.
[41] E. Corvera, O.G. Mouritsen, M.A. Singer and M.J. Zuckermann, Biochim. Biophys. Acta, 1107 (1992) 261.
[42] K. Jørgensen, J.H. Ipsen, O.G. Mouritsen, D. Bennett and M.J. Zuckermann, Biochim. Biophys. Acta, 1062 (1991) 227.
[43] K. Jørgensen, J.H. Ipsen, O.G. Mouritsen, D. Bennett and M.J. Zuckermann, Biochim. Biophys. Acta, 1067 (1991) 241.
[44] K. Jørgensen, J.H. Ipsen, O.G. Mouritsen and M.J. Zuckermann, Chem. Phys. Lipids, 65 (1992) 205.
[45] M.C. Sabra, K. Jørgensen and O.G. Mouritsen, Biochim. Biophys. Acta, 1233 (1994) 89.
[46] D.B. Mountcastle, R.L. Biltonen and M.J. Halsey, Proc. Natl. Acad. Sci. USA, 75 (1978) 4906.
[47] W. van Osdol, Q. Ye, M.L. Johnson and R.L. Biltonen, Biophys. J., 63 (1992) 1011.
[48] M.C. Antunes-Madeira and V.M.C. Madeira, Biochim. Biophys. Acta, 820 (1985) 165.
[49] M.C. Antunes-Madeira and V.M.C. Madeira, Biochim. Biophys. Acta, 861 (1986) 159.
[50] O.G. Mouritsen and M. Bloom, Biophys. J., 46 (1984) 141.
[51] O.G. Mouritsen and M. Bloom, Annu. Rev. Biophys. Biomol. Struct., 22 (1993) 147.
[52] Z. Zhang, M.M. Sperotto, M.J. Zuckermann and O.G. Mouritsen Biochim. Biphys. Acta, 1147 (1993) 154.
[53] M.R. Morrow, J.C. Huschilt, and J.H. Davis, Biochemistry, 24 (1985) 5396.
[54] O.G. Mouritsen, M.M. Sperotto, J. Risbo, Z. Zhang and M.J. Zuckermann, in H.O. Villar (Editor), Adv. Comp. Biol., JAI Press, Greenwich, Connecticut, (in press, 1995).
[55] A. Alonso, C.J. Restall, M. Turner, J.C. Gomez-Fernandez, F.M. Goni and D. Chapman, Biochim. Biophys. Acta, 689 (1982) 283.
[56] T. Hødlnger, K. Mortensen, J.H. Ipsen, J. Lemmich, R. Bauer, and O.G. Mouritsen, Phys. Rev. Lett., 72 (1994) 3911.
[57] R. Lipowsky, Nature, 349 (1991) 1.
[58] W. Helfrich, Z. Naturforsch., 28C (1973) 693.
[59] C. Jeppesen and J.H. Ipsen, Europhys. Lett., 22 (1993) 713.
[60] B. Dammann, H.C. Fogedby, J.H. Ipsen and C. Jeppesen, J. Phys. I Fr., 4 (1994) 1139.
[61] J.H. Ipsen and C. Jeppesen, (preprint, 1995).